

# RSC Advances



This is an *Accepted Manuscript*, which has been through the Royal Society of Chemistry peer review process and has been accepted for publication.

*Accepted Manuscripts* are published online shortly after acceptance, before technical editing, formatting and proof reading. Using this free service, authors can make their results available to the community, in citable form, before we publish the edited article. This *Accepted Manuscript* will be replaced by the edited, formatted and paginated article as soon as this is available.

You can find more information about *Accepted Manuscripts* in the [Information for Authors](#).

Please note that technical editing may introduce minor changes to the text and/or graphics, which may alter content. The journal's standard [Terms & Conditions](#) and the [Ethical guidelines](#) still apply. In no event shall the Royal Society of Chemistry be held responsible for any errors or omissions in this *Accepted Manuscript* or any consequences arising from the use of any information it contains.



## Manipulation and assembly behavior of *Spirulina*-templated microcoils in the electric field†

Xinghao Li,<sup>a</sup> Jun Cai,\*<sup>a</sup> Lili Sun,<sup>a</sup> Yue Yue<sup>a</sup> and Deyuan Zhang<sup>a</sup>

Received 00th January 20xx,  
Accepted 00th January 20xx

DOI: 10.1039/x0xx00000x

www.rsc.org/

This paper investigates the behavior of metallic *Spirulina*-templated microcoil in different alternating electric fields and the feasibility to align multiple microcoils into long conductive microcoil-lines. We used plate-to-plate, plate-to-tip, and tip-to-tip electrodes to produce three different kinds of electric field with a working spacing of 1 mm. The behavior of the microcoils in the AC electric fields was studied based on the force analysis and real-time monitoring. For a single microcoil, it could rotate to orient its major axis parallel with the electric field and then translate towards the nearer electrode if the voltage was suitable. The voltage thresholds for translation in plate-to-plate, plate-to-tip and tip-to-tip electrodes are ~40.5 V, ~38.2 V and ~62 V respectively, which are usually ~10 V higher than those for rotation. For multiple microcoils, they could be directionally aligned and connected one by one in the AC electric field. The simulation results indicate that the polarization of microcoils and the non-uniform electric field strength induced the rotation and translation respectively, and the field gradient around microcoils caused by their helical configurations also contributed. The electric breakover and self-adjustment behavior of the aligned microcoils were also discussed, showing that this technique is applicable to the fabrication of smart conductive composites.

### 1 Introduction

Owing to the complicated and attractive features, three-dimensional helical micro-structures have promising potential for the fabrication of micro-scale electronic devices,<sup>1, 2</sup> heterogeneous integration of micro-electromechanical system<sup>3, 4</sup> and smart tunable materials.<sup>5</sup> Moreover, conductive microcoils can be used in the fields of electromagnetic wave absorbing,<sup>6</sup> energy converter<sup>7</sup> and nuclear magnetic resonance detection.<sup>8</sup> Considering their attractive performance and numerous applications, researchers have developed different ways to fabricate microcoils, such as template-based methods,<sup>2, 6, 9</sup> self-growing methods,<sup>7, 10</sup> 3D direct laser writing (DLW),<sup>4</sup> micro-machining,<sup>3, 11</sup> etc. Among these researches, the template-based and self-growing methods have more advantages in mass-production, yet the DLW and micro-machining methods have merit on the precise control of shapes and dimensions. Targeting the practical application of microcoils,<sup>12</sup> most cases not only require easy mass-production, but also need the

precise manipulation and/or oriented alignment of microcoils, which is quite a challenge.

Up to now, controlling the orientation of micro/nano particles in the fluidic medium has been carried out in various ways.<sup>13-18</sup> Arjmand et al.<sup>19</sup> utilized injection molding technique to achieve the flow-induced orientation of carbon nanotubes to fabricate shielding materials. Nagaoka et al.<sup>14</sup> successfully orientated paramagnetic particles (diameter  $2.20 \pm 0.54 \mu\text{m}$ ) under AC/DC combined magnetic field to prepare complex secondary structures. Scott et al.<sup>17</sup> aligned nanoparticles into microwires by AC electric fields and investigated the ohmic response. Nevertheless, the related work mainly focused on sub-micro or nanoparticles with simple geometries, such as spherical shape,<sup>14, 20</sup> rod shape<sup>18, 21</sup> and flake shape.<sup>22</sup> There is little report on the manipulation and assembly of microcoils. Furthermore, Tottori et al.<sup>4</sup> used magnetic field to control magnetized microcoils as micro-swimmer for cargo transport,

<sup>a</sup>School of Mechanical Engineering and Automation, Beihang University, No.37 Xueyuan Road, Haidian District, Beijing, 100191, China. E-mail: jun\_cai@buaa.edu.cn  
†Electronic Supplementary Information (ESI) available. See DOI: 10.1039/x0xx00000x

and similar researches on magnetic field based manipulation method of microcoils were carried out by Peyer et al.<sup>23</sup> and Gao et al.<sup>24</sup> All these researches are confined to the magnetic microcoils, and the assembly and alignment of helical particles are not mentioned.

For the general non-magnetic microcoils,<sup>2, 6, 12, 25</sup> the manipulation and assembly are more meaningful and attractive due to their broad application. Though the targeting particles are different, electric field-induced alignment has proved to be a feasible and effective method. When particles and suspending medium are subjected to a non-uniform electric field, they could be polarized. The resulting dielectrophoretic (DEP) force on the particles would overcome other forces, including stochastic force originating in the thermal energy of the system and deterministic force such as gravity and viscous forces.<sup>26</sup> Consequently, the particles are either propelled to the region of maximum field intensity (so-called positive DEP) or repelled from it (so-called negative DEP), closely dependent on the effective polarizability of particles and medium. Morgan et al.<sup>26</sup> systematically demonstrated dielectrophoresis of colloidal particles and its extensive application for the characterization, manipulation and separation of particles. Specifically, alternating electric field has been used to accurately direct self-assembly of micro-devices,<sup>27</sup> separate or collect particles with different electronic and structural properties<sup>28, 29</sup> and directionally assemble the particle arrays.<sup>22, 30, 31</sup> Therefore, considering their metallic and conductive properties, we try to make use of the specific alternating electric fields, *i.e.* dielectrophoresis, to control and assemble the complicated helical particles.

In this research, we prepared *Spirulina*-templated conductive microcoils by means of electroless silver plating. Subsequently, the manipulation of a single metallic microcoil and directional assembly of multiple microcoils were carried out in alternating electric fields. Three kinds of electrodes with different configuration were designed to achieve rotation and translation of microcoils. In particular, we illustrated the voltage thresholds of different electrodes for manipulation of the microcoils and visually showed the distribution of DEP force acting on the helical particles. Moreover, multiple microcoils could be assembled into long conductive microcoil-lines in the scale of millimeter. In this dynamic aligning process, we also analysed the current-carrying and self-adjusting capability of microcoil-lines through the voltage variation between plate-to-plate

electrodes, and the feasibility of using alternating electric fields to manipulate and assemble microcoils was validated.

## 2 Experimental

### 2.1 Materials

The microscopic organisms *Spirulina* (*Arthrospira platensis*), with spatially helical structure, are usually cultivated for commercial nutritional products.<sup>32</sup> Here, the *Spirulina* was provided by Tianjin University of Commerce (Tianjin, China) and employed as the biotemplate to fabricate metallic microcoils. **Fig. 1** shows the morphology of original *Spirulina*. In general, the feature size of *Spirulina* are 26–36  $\mu\text{m}$  in diameter ( $D$ ), 5–10  $\mu\text{m}$  in wire diameter ( $d$ ), 100–400  $\mu\text{m}$  in the whole free length ( $L$ ), 4–10 in turn number ( $n$ ), and 43–57  $\mu\text{m}$  in coil pitch ( $l_p$ ). In the experiment, metallic microcoils, *i.e.* silver-coated *Spirulina*, were prepared by electroless silver plating, and the detailed process can be found in our previous work.<sup>25</sup> Moreover, the microcoils were filtrated by the sieve of 300 meshes to eliminate the broken ones and residual silver particles. The absolute ethyl alcohol was used as fluidic medium to disperse the microcoils.

### 2.2 Manipulation and Alignment

We established a custom-made system (as shown in **Fig. 2**), which consisted of a function waveform generator (Agilent, 33522A), an amplifier (XE-50500), a two channel digital storage oscilloscope (RIGOL, DS-5000) and copper electrodes. The function generator could provide a sinusoidal voltage signal  $u = A \cdot \sin(2000\pi t)$  with a constant frequency 1 kHz. Then, the signal was amplified (20 $\times$ ) and output voltage

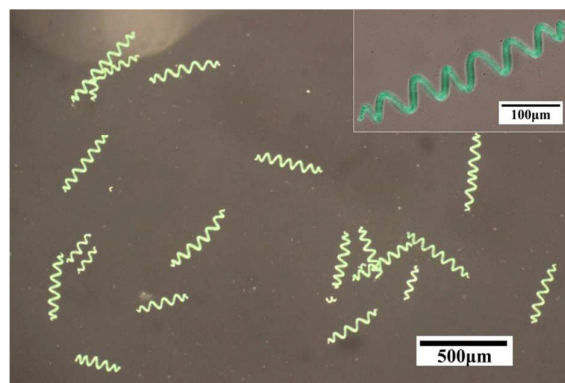


**Fig. 1** Optical microscopic image of original *Spirulina*.

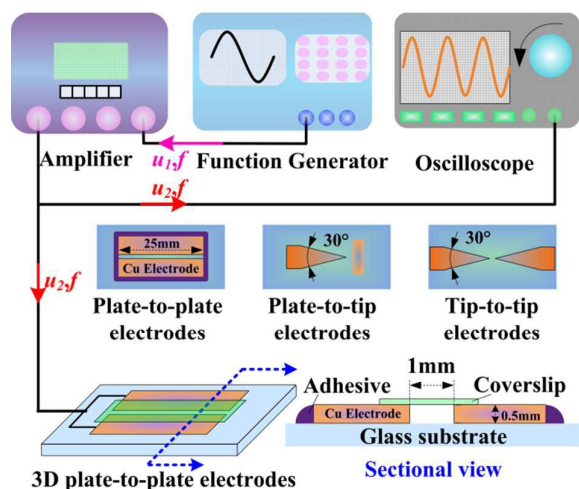


**Fig. 2** The schematic illustration of set-up for manipulation and alignment of microcoils.

was detected in real time by the oscilloscope. Three kinds of electrodes with different feature configuration, including plate-to-plate, plate-to-tip and tip-to-tip, were fabricated by wire electrical discharge machining (WEDM, DK7720), which can avoid undesired deformation. Also, the end of a tip electrode was machined into  $30^\circ$  (with  $\pm 1^\circ$  error). All the surfaces of copper electrodes were grinded with abrasive papers (1000 mesh) to remove oxidation layer. Furthermore, the electrodes were fixed on a glass slide (75 mm in length and 25 mm in width) and the spacing between two electrodes was about 1 mm in width.

For the manipulation of a single microcoil, the gap was filled up with medium (absolute ethyl alcohol) by using an injector, and a glass micropipette was applied to adjust the initial position of particles. Also, the selected microcoils were about  $\sim 250$   $\mu\text{m}$  in length and initial position was kept nearly the same to reduce error. For the alignment of multiple microcoils, the particles were randomly dispersed in the medium by stirring them at a low rate of 80 rpm for 10 min at room temperature. Then 8–10  $\mu\text{L}$  suspension was filled into the gap between two electrodes. A small glass coverslip was placed on the electrodes to prevent the volatilization of alcohol and external airflow disturbance.

### 2.3 Real-time Voltage Measurement during Alignment Process

The real-time measurement system was built to record the dynamic voltage variation during the alignment process (Fig. 3). The oscilloscope was in parallel connection with the plate electrodes to capture the image data of real-time voltage

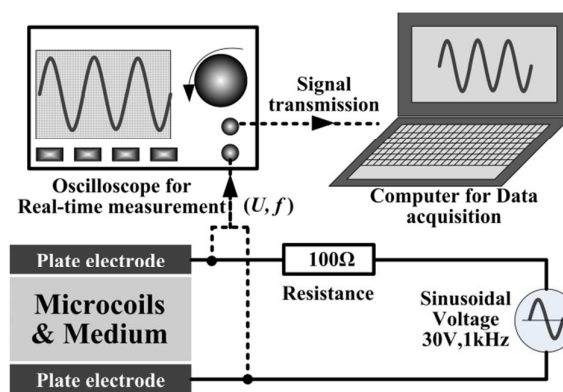


**Fig. 3** Structural schematic of a real-time voltage measurement system. Dot lines show the signal transmission.

variation. The time scale of one frame was 6 ms and an interval between two frames was set as the minimum 1 ms. With the bundled software, the real-time voltage data of every frame could be acquired and processed. Furthermore, we used a 100 ohm resistance in series with one of the electrodes to avoid high current and protect the circuit.

### 2.4 Microscopic Observation

The morphology of metallic silver-coated *Spirulina* was characterized using scanning electron microscopy (JSM-6010LA, JEOL, Ltd.) and the composition analysis was conducted by energy dispersive spectrometer (EDS). Also, the crystal structure of silver coating was examined by utilizing X-ray diffraction (XRD, Rigaku RINT-Ultima). Optical microscopy (Olympus, BX51) with digital camera (Canon, 600D) was applied to observe the motion of a single microcoil and alignment behavior of multiple microcoils.

## 3 Results and Discussion

### 3.1 Metallic Microcoils Characterization

The SEM of *Spirulina* after electroless plating is shown in Fig. 4a, from which we can see that its helical configuration was perfectly remained, and the coating on *Spirulina* template was homogeneous. The EDS results (Fig. 4b) illustrate that the principal components of microcoils were silver, carbon and oxygen, and silver was the key element (up to 90 wt.%). Moreover, Fig. 4c shows the XRD of microcoils. We note that five major peaks appeared at  $38.1^\circ$ ,  $44.4^\circ$ ,  $64.2^\circ$ ,  $77.4^\circ$  and  $81.5^\circ$  in diffraction angle  $2\theta$ , which were consistent with face-centered-cubic (FCC) structured crystalline silver. This result further confirmed that the microcoil was coated with silver.

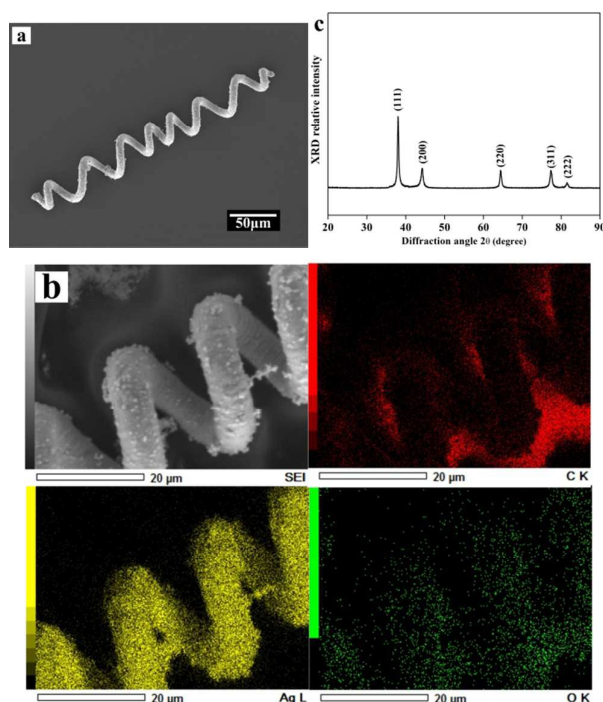


**Fig. 4** Characterization of the silver coated *Spirulina*-templated microcoils. (a) SEM image of a single silver coated microcoil. (b) Elemental mapping image for the microcoil through EDS analysis. The red, yellow and green points represent the carbon, silver and oxygen element, respectively. (c) XRD pattern of the silver coating of microcoils.

### 3.2 Manipulation of a Single Microcoil

**Fig. 5** shows the exact position and posture of a microcoil at different time points, including original state without applying electric field, after rotation and translation in AC electric fields. (see as well as **ESI†** video S1 to 3). The major axis of microcoils was almost perpendicular to the field in the beginning. Both electric field amplitude  $E$  and frequency  $f$  have effects on DEP force and motion of particles.<sup>26, 33</sup> For simplifying the manipulation process, the frequency was set as a constant 1 kHz.<sup>22, 30, 34</sup> With voltage increasing from zero, microcoils in the electric field would firstly rotate at a specific voltage value till the major axis parallel with the electric field. Then, the voltage continued to increase and the microcoils directionally translated towards the nearer electrode. Finally, the particle would contact the electrode as a new part. It indicates that the specific AC electric fields could be applied to manipulate and orient a single microcoil.

The mechanism is that metallic microcoils, dispersed in the absolute ethyl alcohol, could be polarized in the time-varying

and space-varying electric field, resulting in the formation of induced dipoles moment. The symmetric line of the gap could be regarded as the boundary, and DEP force on each side of the boundary would point to the region of higher field magnitude. Additionally, the microcoils are anisotropic with a high respect ratio of 5-20. Each end of the particles would experience an equal and opposite force tending to align its major axis parallel with the field, *i.e.* the microcoil experiences a torque. However, when the major axis of microcoils was initially parallel with electric field, the rotation would not happen. The main reason seems to be that the dipole moment of microcoils depends on its orientation with respect to the electric field. When the major axis orients in the field direction, the components of electric field along other axes are about zero, and the effective torque would vanish.<sup>26</sup> After rotation, the microcoil would be driven towards the electrode predominantly by DEP force along major axis. In particular, as for the plate-to-plate or tip-to-tip electrodes, if the major axis of microcoils is parallel with the electric field and the ends of particles are just equidistant from both electrodes, the microcoil theoretically would not translate towards either electrode, which is a rare and unstable situation. This is mainly due to the fact that the DEP forces acting on two ends of particles are a pair of equal and opposite forces along with the major axis.

Furthermore, the time-averaged force  $F_{DEP}$  on the particle was given by the analytical expression:<sup>26, 33, 35</sup>

$$\langle F_{DEP} \rangle = \frac{1}{4} v \operatorname{Re}[\tilde{\alpha}] \nabla |\mathbf{E}|^2 \quad (1)$$

where  $v$  (in  $\text{m}^3$ ) is the volume of a helical particle,  $\tilde{\alpha}$  is complex polarisability and  $\nabla |\mathbf{E}|^2$  (in  $\text{V}^2 \cdot \text{m}^{-3}$ ) is the gradient of electric field magnitude squared. The microcoil is anisotropic and could be approximated to a cylindrical particle with high aspect ratio,<sup>26</sup> and half lengths along the three axes (**Fig.6 inset**) could be written as  $a_n$  ( $n=1, 2$  and  $3$ ). According to the geometrical configuration features of metallic microcoils, the whole particle generally shows the condition  $a_1 > a_2 = a_3$ , and the depolarizing factor  $A_n$  along different axes could be given by<sup>26</sup>

$$A_1 = \frac{e^2 - 1}{2e^3} \left( 2e - \ln \frac{1+e}{1-e} \right) \quad (2)$$

$$A_2 = A_3 = \frac{1 - e^2}{4e^3} \left( \frac{2e}{1 - e^2} - \ln \frac{1+e}{1-e} \right) \quad (3)$$

where  $e = \sqrt{1 - (a_2/a_1)^2}$  and it is dependent on the aspect ratio of particles. For the microcoils of various sizes,  $e$  is about 0.983~0.998. So the value of  $A_1$  varies from 0.007 to 0.048,

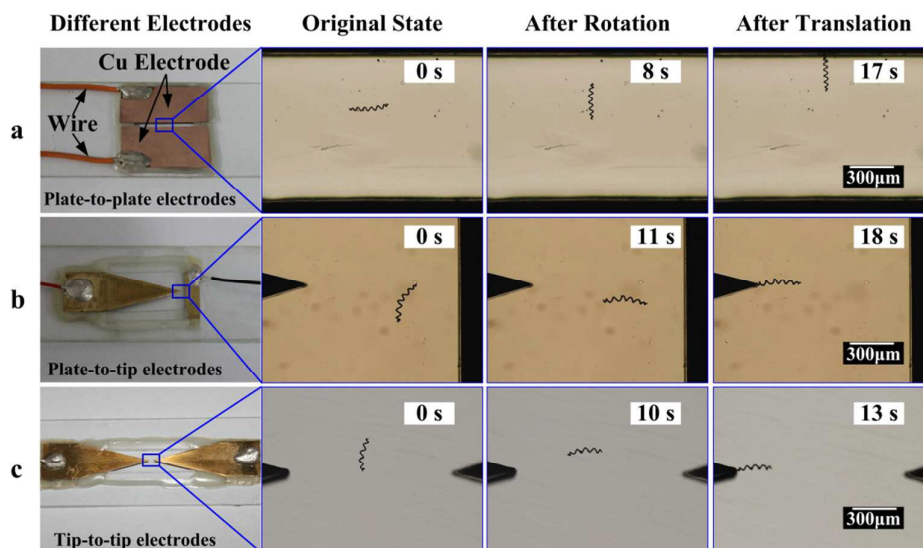


**Fig. 5** Manipulation of a single microcoil in electric fields generated by three different electrodes configurations: (a) plate-to-plate electrodes; (b) plate-to-tip electrodes; (c) tip-to-tip electrodes.

while  $A_2$  and  $A_3$  from 0.476 to 0.496. It seems that depolarizing factor  $A_I$  (along the major axis) tends to zero, while both  $A_2$  and  $A_3$  are about 0.5. The effective polarizability is given by  $\tilde{\alpha}_n = 3\epsilon_m \tilde{K}_n$  ( $n=1, 2$  and  $3$ ).  $\tilde{K}_n$  is equivalent to the Clausius-Mossotti factor and could be written as<sup>26</sup>

$$\tilde{K}_n = \frac{\tilde{\epsilon}_p - \tilde{\epsilon}_m}{3(A_n(\tilde{\epsilon}_p - \tilde{\epsilon}_m) + \tilde{\epsilon}_m)} \quad (4)$$

where  $\tilde{\epsilon}_p$  and  $\tilde{\epsilon}_m$  are the complex permittivity of particle and suspending medium respectively.

**Fig. 6** shows the values for the real part of the Clausius-Mossotti factor along three axes as a function of frequency. The real part of  $\tilde{K}_1$  (about  $10^{12}$  at 1 kHz) is far higher than that of

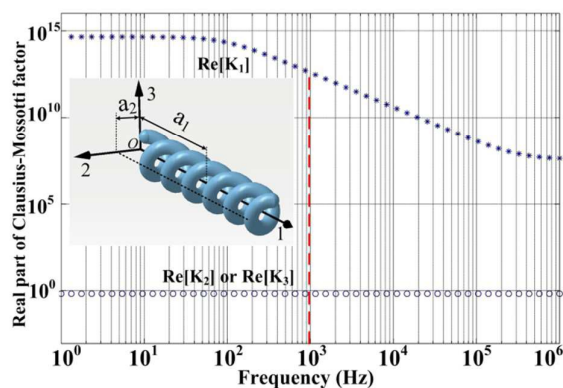


**Fig. 6** Calculated values for the real part of Clausius-Mossotti factor along three axes as a function of frequency. Inset shows the 3D model of a *Spirulina*-templated microcoil.

$\tilde{K}_2$  and  $\tilde{K}_3$  (about 100 at 1 kHz). Furthermore, the Clausius-Mossotti factor along major axis monotonously decreases against frequency ( $\leq 1$  MHz), but still maintains larger than that along the other two axes. It indicates that  $F_{DEP}$  along major axis always remains dominant at both low and high frequency. This phenomenon is mainly due to the fact that the complex permittivity<sup>36</sup> of metallic microcoil ( $\tilde{\epsilon}_p = 10^9 \epsilon_0 - i[6.06 \times 10^7]/\omega$ ) is significantly different from that of the suspending medium absolute ethyl alcohol ( $\tilde{\epsilon}_m = 25.7 \epsilon_0 - i[1.35 \times 10^7]/\omega$ ), resulting in the particles being much more polarizable than the medium. Therefore, the metallic microcoils would move towards the higher field magnitude, *i.e.* the positive DEP.

For the targeted manipulation and directed assembly of helical particles in different AC electric fields, much attention should be paid to the key voltage thresholds<sup>37</sup>, at which the microcoils begin to rotate and translate. **Fig. 7** shows the voltage threshold for rotation and translation of a single microcoil in different AC electric fields with spacing of 1 mm. The particles were placed nearly in the middle of the spacing between two electrodes and the major axis was almost perpendicular to the electric field. It is mainly because the gradient of electric field strength decays away from the electrode surface and DEP force presents minimum value in the middle. For the three electrodes of different configurations, each voltage threshold for rotation is about  $\sim 10$  V lower than

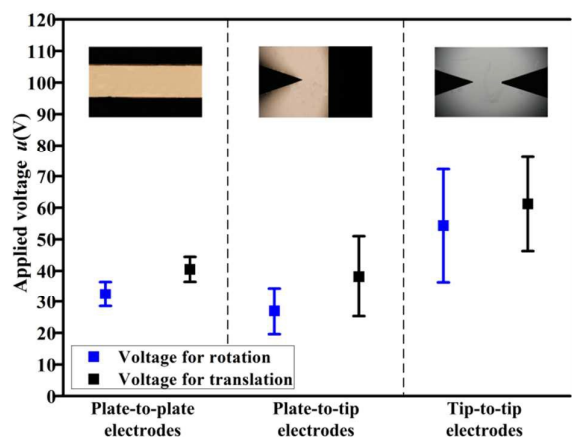


**Fig. 7** The voltage thresholds for rotation and translation of a single microcoil in different AC electric fields with spacing of 1 mm. The insets show different electrodes configuration.

that for translation. The voltage threshold for translation in tip-to-tip electrodes is the highest ( $\sim 62$  V), yet the value in plate-to-plate electrodes is  $\sim 40.5$  V, which is nearly equal to that in plate-to-tip electrodes ( $\sim 38.2$  V). The possible reason is that DEP force, *i.e.*  $\nabla|E|^2$ , in tip-to-tip electrodes decays most rapidly away from tip electrode and reaches minimum in the middle of the gap,<sup>38</sup> and the voltage needs to be higher to generate a comparable  $F_{DEP}$  to drive microcoils. Also, for tip-to-tip electrodes,  $\nabla|E|^2$  largely depends on the position and even a slight change of original position in the experiment may cause different voltage threshold values. Therefore, the variation range of voltage thresholds for tip-to-tip electrodes is wide.

Additionally, the voltage thresholds for three electrodes would decline with the increase of microcoil concentration in the medium on account of the interaction of multiple particles.<sup>26,39</sup>

To further study the force mechanism on the microcoils in the AC electric field, the distribution of  $\nabla|E|^2$  (in  $V^2 \cdot m^{-3}$ ) around microcoils in different situation was simulated, as shown in **Fig. 8**. It is clear that the electric fields differ much among the three situations, and the electric field magnitude around microcoils varies dramatically, which is completely different from that around the rod-like particles<sup>21,33</sup> and micro spheres.<sup>35</sup> This difference is mainly due to the helical shape and complicated configuration. The gradient  $\nabla|E|^2$  at the end of the microcoils can reach  $10^{15} \sim 10^{16} V^2 \cdot m^{-3}$ , which is much higher than that of regular particles and may be beneficial for the assembly and alignment of microcoils.

For the plate-to-plate electrodes, when the major axis of microcoils was parallel with the electric field,  $\nabla|E|^2$  around the left end of microcoil showed the maximum value  $\sim 3.5 \times 10^{16} V^2 \cdot m^{-3}$ , and it kept changing with the position and posture of microcoil in the electric field. After translation, the microcoil would physically connect the plate electrode and its major axis kept perpendicular to the electrode. Then the microcoil would act as a new tip electrode, and the local  $\nabla|E|^2$  at the far end increased to  $\sim 6.0 \times 10^{16} V^2 \cdot m^{-3}$ , which is favourable for the following continuous alignment of multiple microcoils. Furthermore, similar situations were also found for the other two electrode configurations.

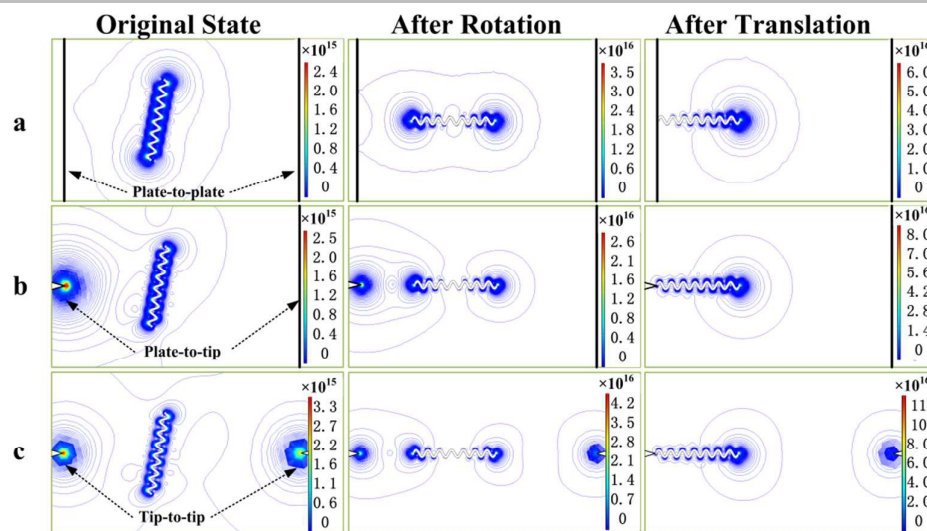


**Fig. 8** The distribution of  $\nabla|E|^2$  (in  $V^2 \cdot m^{-3}$ ) around microcoils in different situation: (a) plate-to-plate electrodes; (b) plate-to-tip electrodes; (c) tip-to-tip electrodes. The solid blue lines are the contour line of  $\nabla|E|^2$ .

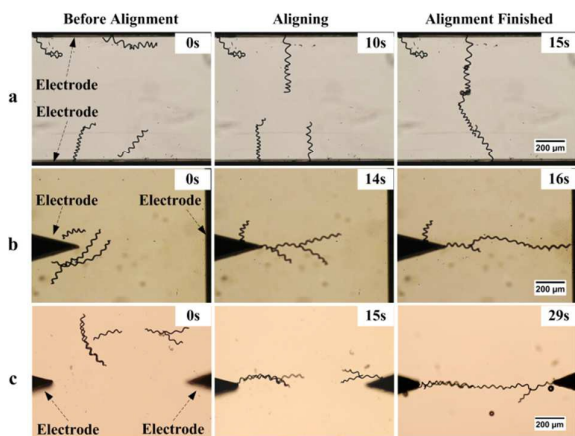


**Fig. 9** Assembly and alignment of multiple microcoils into long lines in different electric fields: (a) plate-to-plate electrodes; (b) plate-to-tip electrodes; (c) tip-to-tip electrodes.

Comparing these three AC electric fields, the plate-to-plate electrodes are more stable for manipulation and have the maximum effective area, which is suitable for batch alignment or assembly. The tip electrodes may be used to separate the single particle accurately.

### 3.3 Assembly Behavior of Multiple Microcoils

#### 3.3.1 Alignment into Long Microcoil-line

The microcoil-line could be formed and aligned to fill the gap between two electrodes (as shown in Fig. 9, see as well as ESI† Video S4 to 6), when suitable voltage was employed (20 V for plate-to-plate electrodes, 22 V for plate-to-tip and 30 V for tip-to-tip). The microcoils close to an electrode would be propelled and connected the electrode as mentioned above. Then they could be assembled one by one from two edges to the middle

(for plate-to-plate electrodes and tip-to-tip electrodes) or from one electrode to the other (for plate-to-tip electrodes) in less than 30 s. Some bubbles could be found at the junction of two microcoils during the alignment process. This mainly results from the contact resistance and large current intensity at the touch point, which may lead to local ablation and thermal decomposition of the *Spirulina* template. Additionally, the longer microcoil-lines with 5mm in length have also been successfully achieved through the wider AC electric field (300 V/mm, 1 kHz, see ESI† Video S7). It indicates that this technique can be scaled up for macroscopic fabrication of microcoil-based materials.

#### 3.3.2 Voltage Variation during Dynamic Alignment Process

The voltage between plate-to-plate electrodes was measured in real time when the microcoils assembly was carried out. Fig. 10 shows the voltage variation during the dynamic alignment process. When there was no signal input, the voltage between two electrodes remained at zero (Fig. 10b). Then, the alternating voltage of 30 V (1 kHz) was applied and the sinusoidal wave (Fig. 10c) could be measured, during which batch microcoils were efficiently aligned and assembled (as shown in ESI† Video S4). The sinusoidal voltage would keep stable for a few seconds till the alignment was completed. Then the voltage would abruptly decrease to about zero on account of the breakover of two electrodes (as shown in Fig. 10d), implying that the complete conductive networks have been formed. Yet the voltage between two electrodes may still have irregular fluctuation, (as shown in Fig. 10e and Fig. 10f). This is caused by the joule heat release<sup>40</sup> and small explosion at the touch point of two microcoils, which would separate the

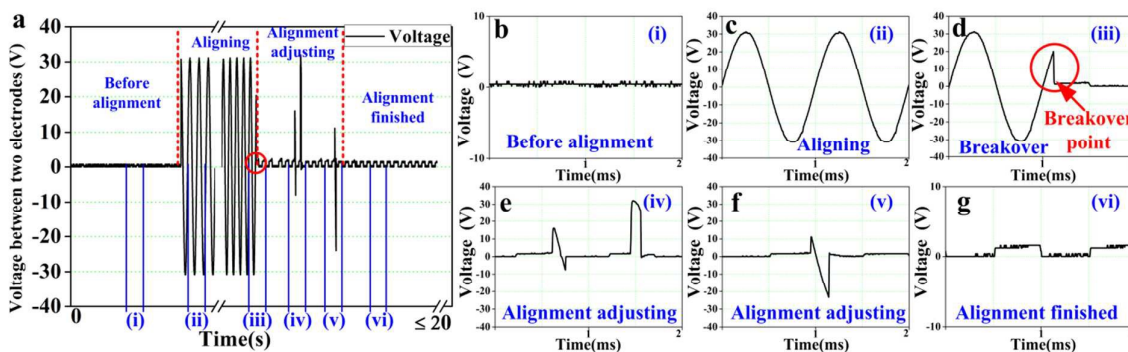


**Fig. 10** Voltage variation between plate-to-plate electrodes during the dynamic alignment process. (a) The whole assembly process in less than 20s. (b-g) Details of voltage variation during the alignment process in the scale of 2ms.

physically connected particles and break the circuit. Consequently, the voltage between electrodes rapidly responded and increased, so as to impel the re-assembly of microcoils into continuous wires again. This self-adjustment would occur repeatedly until stable conductive networks were formed between the two electrodes, and the voltage value would remain at about zero (Fig. 10g). Since the input voltage was remained during the whole assembly process, the nearly zero voltage between the electrodes indicates that the achieved conductive networks own low resistance, which is determined by the intrinsic resistance of conductive particles and the contact resistance between connected particles. Considering the steady conductive performance, this technique could be used for the fabrication of highly reliable smart conductive composites.

#### 4 Conclusion

We demonstrated that alternating electric field could be applied to manipulate metallic microcoils and directionally align multiple microcoils. For a single microcoil, it would be polarized and subjected to the positive DEP in AC electric fields since its polarizability is much bigger than that of medium (absolute ethyl alcohol). The microcoil would always rotate to align its major axis parallel with electric field, and then translate towards the nearer electrode. The voltage threshold for particles' rotation and translation in different electric fields was elaborated, and the working mechanism was analyzed by means of simulation, which showed that polarization of microcoils and non-uniform gradient of field magnitude squared  $\nabla|E|^2$  were the main causes. Furthermore, multiple microcoils could be directionally aligned one by one from two edges to the middle (for plate-to-plate and tip-to-tip electrodes) or from one electrode to the other (for plate-to-tip electrodes). In addition, the multiple microcoil-lines performed re-assembling and current-carrying capability in the electric field. This technology shows potential for the fabrication of highly reliable smart conductive composites.

#### Acknowledgements

This work was supported by the National Natural Science Foundation of China (Grant No. 51322503 and No. 51275025) and the Fundamental Research Funds for the Central Universities.

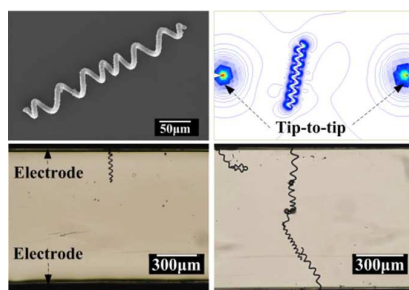
#### Notes

The authors declare no competing financial interest.

#### Reference

- 1 J. Park and M. Allen, *Journal of Micromechanics and Microengineering*, 1998, **8**, 307.
- 2 K. Kamata, S. Suzuki, M. Ohtsuka, M. Nakagawa, T. Iyoda and A. Yamada, *Advanced Materials*, 2011, **23**, 5509-5513.
- 3 K. Jolic, M. Ghantasala, J. Hayes and H. Jin, *Journal of Micromechanics and Microengineering*, 2003, **13**, 782.
- 4 S. Tottori, L. Zhang, F. Qiu, K. K. Krawczyk, A. Franco - Obregón and B. J. Nelson, *Advanced materials*, 2012, **24**, 811-816.
- 5 K. Yoshimura, K. Nakano, T. Miyake, Y. Hishikawa, C. Kuzuya, T. Katsuno and S. Motojima, *carbon*, 2007, **45**, 1997-2003.
- 6 K. Kamata, Z. Piao, S. Suzuki, T. Fujimori, W. Tajiri, K. Nagai, T. Iyoda, A. Yamada, T. Hayakawa and M. Ishiwara, *Scientific reports*, 2014, **4**.
- 7 S. Motojima and X. Chen, *Bulletin of the Chemical Society of Japan*, 2007, **80**, 449-455.
- 8 C. Massin, G. Boero, F. Vincent, J. Abenhaim, P.-A. Besse and R. Popovic, *Sensors and Actuators A: Physical*, 2002, **97**, 280-288.
- 9 B. Chen, T. Zhan, Z. Lian and D. Zhang, *Science in China Series E: Technological Sciences*, 2008, **51**, 591-597.
- 10 H.-F. Zhang, C.-M. Wang, E. C. Buck and L.-S. Wang, *Nano Letters*, 2003, **3**, 577-580.
- 11 C. N. LaFratta, J. T. Fourkas, T. Baldacchini and R. A. Farrer, *Angewandte Chemie International Edition*, 2007, **46**, 6238-6258.
- 12 Z. Ren and P.-X. Gao, *Nanoscale*, 2014, **6**, 9366-9400.
- 13 M. Mittal and E. M. Furst, *Advanced Functional Materials*, 2009, **19**, 3271-3278.
- 14 Y. Nagaoka, H. Morimoto and T. Maekawa, *Langmuir*, 2011, **27**, 9160-9164.
- 15 Y.-C. Chao, W.-H. Huang, K.-M. Cheng and C. Kuo, *ACS applied materials & interfaces*, 2014, **6**, 4338-4345.
- 16 X. Chen, T. Saito, H. Yamada and K. Matsushige, *Applied physics letters*, 2001, **78**, 3714-3716.
- 17 S. O. Lumsdon and D. M. Scott, *Langmuir*, 2005, **21**, 4874-4880.
- 18 M. Collet, S. Salomon, N. Y. Klein, F. Seichepine, C. Vieu, L. Nicu and G. Larrieu, *Advanced Materials*, 2015, **27**, 1268-1273.

- 19 M. Arjmand, M. Mahmoodi, G. A. Gelves, S. Park and U. Sundararaj, *Carbon*, 2011, **49**, 3430-3440.
- 20 O. D. Velev and K. H. Bhatt, *Soft Matter*, 2006, **2**, 738-750.
- 21 K. A. Rose, J. A. Meier, G. M. Dougherty and J. G. Santiago, *Phys. Rev. E*, 2007, **75**, 011503.
- 22 G. Johnsen, M. Knaapila, Ø. Martinsen and G. Helgesen, *Composites Science and Technology*, 2012, **72**, 1841-1847.
- 23 K. E. Peyer, L. Zhang and B. J. Nelson, *Nanoscale*, 2013, **5**, 1259-1272.
- 24 W. Gao, X. Feng, A. Pei, C. R. Kane, R. Tam, C. Hennessy and J. Wang, *Nano letters*, 2013, **14**, 305-310.
- 25 J. Cai, M. Lan, D. Zhang and W. Zhang, *Applied Surface Science*, 2012, **258**, 8769-8774.
- 26 H. Morgan and N. G. Green, *AC electrokinetics: colloids and nanoparticles*, Research Studies Press, 2003.
- 27 S. W. Lee and R. Bashir, 2005.
- 28 R. Krupke, S. Linden, M. Rapp and F. Hennrich, *Advanced materials*, 2006, **18**, 1468-1470.
- 29 K. H. Bhatt, S. Grego and O. D. Velev, *Langmuir*, 2005, **21**, 6603-6612.
- 30 M. Knaapila, O. T. Rømoen, E. Svåsand, J. P. Pinheiro, Ø. G. Martinsen, M. Buchanan, A. T. Skjeltorp and G. Helgesen, *ACS applied materials & interfaces*, 2011, **3**, 378-384.
- 31 A. Kadimi, K. Benhamou, Z. Ounaies, A. Magnin, A. Dufresne, H. Kaddami and M. Raihane, *ACS applied materials & interfaces*, 2014, **6**, 9418-9425.
- 32 E. Becker, *Biotechnology advances*, 2007, **25**, 207-210.
- 33 S. Raychaudhuri, S. A. Dayeh, D. Wang and E. T. Yu, *Nano letters*, 2009, **9**, 2260-2266.
- 34 C. Martin, J. Sandler, A. Windle, M.-K. Schwarz, W. Bauhofer, K. Schulte and M. Shaffer, *Polymer*, 2005, **46**, 877-886.
- 35 O. D. Velev, S. Gangwal and D. N. Petsev, *Annual Reports Section "C" (Physical Chemistry)*, 2009, **105**, 213-246.
- 36 S. Gangwal, O. J. Cayre and O. D. Velev, *Langmuir*, 2008, **24**, 13312-13320.
- 37 H. Morgan and N. G. Green, *Journal of Electrostatics*, 1997, **42**, 279-293.
- 38 H. Ding, J. Shao, Y. Ding, W. Liu, H. Tian and X. Li, *ACS applied materials & interfaces*, 2015.
- 39 T. Jones and M. Washizu, *Journal of Electrostatics*, 1996, **37**, 121-134.
- 40 T. B. Jones and T. B. Jones, *Electromechanics of particles*, Cambridge University Press, 2005.



Manipulation and assembly of complicated metallic *Spirulina*-templated microcoils can be achieved through alternating electric fields.